



Microstructure, martensitic transformation and mechanical properties of Ni–Mn–Sn alloys by substituting Fe for Ni

Chang-long TAN¹, Zhi-cheng FENG¹, Kun ZHANG², Ming-yang WU³, Xiao-hua TIAN¹, Er-jun GUO²

1. College of Applied Science, Harbin University of Science and Technology, Harbin 150080, China;
2. School of Materials Science and Engineering, Harbin University of Science and Technology, Harbin 150080, China;
3. Key Laboratory of National and Local United Engineering for High-Efficiency Cutting & Tools, Harbin University of Science and Technology, Harbin 150080, China

Received 9 December 2016; accepted 21 July 2017

Abstract: The effects of partial substitution of Fe element for Ni element on the structure, martensitic transformation and mechanical properties of $\text{Ni}_{50-x}\text{Fe}_x\text{Mn}_{38}\text{Sn}_{12}$ ($x=0$ and 3%, molar fraction) ferromagnetic shape memory alloys were investigated. Experimental results indicate that by substitution of Fe for Ni, the microstructure and crystal structure of the alloys change at room temperature. Compared with $\text{Ni}_{50}\text{Mn}_{38}\text{Sn}_{12}$ alloy, the martensitic transformation starting temperature of $\text{Ni}_{47}\text{Fe}_3\text{Mn}_{38}\text{Sn}_{12}$ alloy is decreased by 32.5 K. It is also found that martensitic transformation occurs over a broad temperature window from 288.9 to 352.2 K. It is found that the mechanical properties of Ni–Mn–Sn alloy can be significantly improved by Fe addition. The $\text{Ni}_{47}\text{Fe}_3\text{Mn}_{38}\text{Sn}_{12}$ alloy achieves a maximum compressive strength of 855 MPa with a fracture strain of 11%. Moreover, the mechanism of the mechanical property improvement is clarified. Fe doping changes the fracture type from intergranular fracture of $\text{Ni}_{50}\text{Mn}_{38}\text{Sn}_{12}$ alloy to transgranular cleavage fracture of $\text{Ni}_{47}\text{Fe}_3\text{Mn}_{38}\text{Sn}_{12}$ alloys.

Key words: Ni–Mn–Sn alloys; martensitic transformation; mechanical properties; ferromagnetic shape memory alloys

1 Introduction

The fact that the off-stoichiometric $\text{Ni}_2\text{Mn}_{1+x}\text{X}_{1-x}$ ($\text{X}=\text{In}, \text{Sb}$ or Sn) ferromagnetic shape memory alloys (FSMAs) undergo martensitic transformation (MT) was reported by SUTOU et al [1] for the first time. Later, Ni–Mn–Sn shape memory alloy has been widely investigated [2–9]. Researchers found that compared to Ni–Mn–Ga FSMAs, Ni–Mn–Sn FSMAs showed a different mechanism of magnetic field-induced reverse martensitic transformation [1,2,10]. Under an external magnetic field, Ni–Mn–Sn FSMAs undergo the martensitic transformation, rather than the martensitic twin variant rearrangement [11,12]. In addition, this kind of FSMAs are subjected to a metamagnetic transition from the weak magnetic martensite to strong ferromagnetic austenite under an external magnetic field, and a large magnetization difference (ΔM) between

transforming phases can be observed. Thus, the FSMAs showed a lot of unique and amazing physical properties, such as magnetic shape memory effect, magneto-resistance, magnetothermal conductivity, magnetocaloric effect [2,5], elastocaloric effect [13], and exchange bias [8,9]. These fantastic physical properties make it a good candidate for multifunctional materials in many fields.

In recent years, most researchers focus on developing the functional properties of Ni–Mn–Sn magnetic shape memory alloys. However, such an alloy is usually too brittle for practical use. Little information and rare approaches were adopted to improve the mechanical properties of Ni–Mn–Sn magnetic shape memory alloys. Some researchers expect to improve the mechanical properties by reducing the manganese content of the alloys. Nevertheless, the reduction of manganese content will directly reduce the magnetic properties of alloys. It is essential that the reverse

Foundation item: Projects (51471064, 51301054) supported of the National Natural Science Foundation of China; Project (1253-NCET-009) supported by the Program for New Century Excellent Talents, China; Project (1251G022) supported by Program for Youth Academic Backbone in Heilongjiang Provincial University, China; Project (12541138) supported by Scientific Research Fund of Heilongjiang Provincial Education Department, China

Corresponding author: Er-jun GUO; Tel: +86-451-86390008; E-mail: guoerjun@126.com

DOI: 10.1016/S1003-6326(17)60249-8

martensitic transformation can be driven by a weak external magnetic field. Namely, a large ΔM should be obtained. Now, researchers have found that by substituting a small amount of Co for Ni, a local ferromagnetic structure was formed in the antiferromagnetic matrix and the magnetization of the high temperature phase was significantly improved. So, a large ΔM was obtained [14]. Co and Fe are both magnetic atoms. Fe addition can also introduce the second phase [15–18]. So, we logically expect to improve the mechanical properties without sacrificing the magnetic properties of Ni–Mn–Sn magnetic shape memory alloys by partial substituting of Fe element for Ni element.

On the other hand, as a typical ferromagnetic shape memory alloy, the Curie temperature of the austenite should be higher than the temperature of MT. For this reason, to tune the MT temperature in a wide temperature region is necessary. Meanwhile, the martensitic transformation with a broad temperature window makes the alloys easier to be transported and to have greater application value.

In the present work, the influence of Fe addition in $\text{Ni}_{50-x}\text{Fe}_x\text{Mn}_{38}\text{Sn}_{12}$ ($x=0$ and 3%, molar fraction) alloys on the microstructure, martensitic transformation and mechanical properties was focused on. The improvement of mechanical properties is expected to provide a prerequisite for the practical application of Ni–Mn–Sn FSMAs.

2 Experimental

Polycrystalline alloys with $\text{Ni}_{50-x}\text{Fe}_x\text{Mn}_{38}\text{Sn}_{12}$ ($x=0$ and 3%, molar fraction) nominal composition were prepared by induction melting elemental Ni (99.99%), Fe (99.99%), Mn (99.9%) and Sn (99.99%) in nonconsumable electrode arc-melting furnace under an argon atmosphere. The obtained sample ingots were annealed in vacuum quartz tubes at 1123 K for 24 h, subsequently quenched in ice water for homogeneity. The microstructure of the alloys was studied using a scanning electron microscopy (SEM). And the chemical compositions were determined by means of energy X-ray dispersive spectroscopy (EDS) equipped on SEM. Phase identification and crystal structure were determined by X-ray diffraction at room temperature. The martensitic transformation behavior of the samples was determined by differential scanning calorimetry (DSC) using a Perkin–Elmer diamond calorimeter with a heating and cooling rate of 10 K/min. The mechanical experiment was performed at room temperature on an Instron 5569 testing system at a crosshead displacement speed of 0.1 mm/min, and the size of the sample was $d3 \text{ mm} \times 6 \text{ mm}$. The samples were compressed to fracture. And

fractography was observed by SEM to study the dominant fracture behavior.

3 Results and discussion

3.1 Microstructure

Figure 1 shows the back scattered electron (BSE) micrographs of the annealed $\text{Ni}_{50-x}\text{Fe}_x\text{Mn}_{38}\text{Sn}_{12}$ ($x=0$ and 3%, molar fraction) alloys. The alloy exhibits a single phase state without Fe addition, as shown in Fig. 1(a). With 3% Fe addition, trace amount of γ precipitates (in dark contrast) appear in the matrix (in light contrast), as shown in Fig. 1(b). It is found that γ phase is mainly formed at the grain boundaries. The compositions of the matrix alloy and γ phase in $\text{Ni}_{50-x}\text{Fe}_x\text{Mn}_{38}\text{Sn}_{12}$ ($x=0$ and 3%) alloys are listed in Table 1. The highest content of Fe in the matrix is 3.1%, when x is 3% (molar fraction). On the other hand, the γ phase contains a lower content of Sn but much higher content of Fe (11.9%, molar fraction). Furthermore, this probably implies that the γ phase is in a solid solution state rather than an intermetallic which exhibits a specific composition.

Figure 2 shows the X-ray diffraction pattern of $\text{Ni}_{50-x}\text{Fe}_x\text{Mn}_{38}\text{Sn}_{12}$ ($x=0$ and 3%) alloys. The alloy

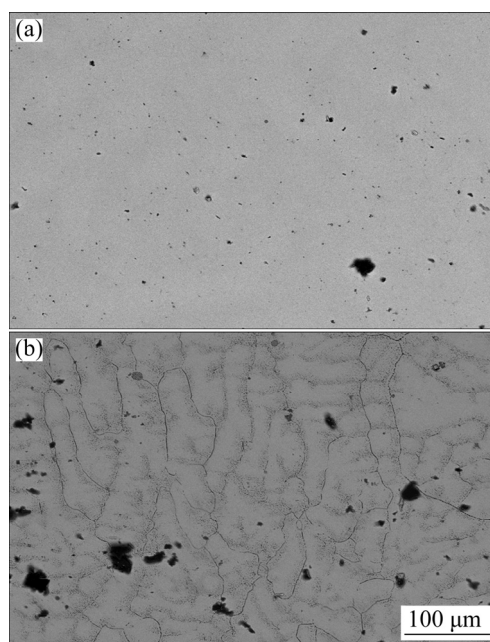


Fig. 1 Backscattered electron images of $\text{Ni}_{50}\text{Mn}_{38}\text{Sn}_{12}$ (a) and $\text{Ni}_{47}\text{Fe}_3\text{Mn}_{38}\text{Sn}_{12}$ (b) alloys

Table 1 EDS results of annealed $\text{Ni}_{50}\text{Mn}_{38}\text{Sn}_{12}$ and $\text{Ni}_{47}\text{Fe}_3\text{Mn}_{38}\text{Sn}_{12}$ alloys (molar fraction, %)

Alloy	Matrix				Second phase			
	Ni	Mn	Sn	Fe	Ni	Mn	Sn	Fe
$\text{Ni}_{50}\text{Mn}_{38}\text{Sn}_{12}$	49.7	38.6	11.7	–	–	–	–	–
$\text{Ni}_{47}\text{Fe}_3\text{Mn}_{38}\text{Sn}_{12}$	47.1	37.5	12.7	2.7	39.5	41.9	6.7	11.9

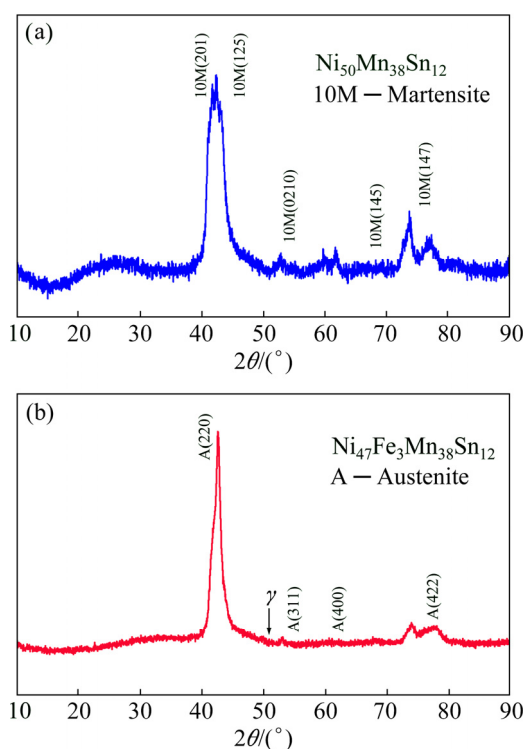


Fig. 2 XRD patterns of $\text{Ni}_{50}\text{Mn}_{38}\text{Sn}_{12}$ (a) and $\text{Ni}_{47}\text{Fe}_3\text{Mn}_{38}\text{Sn}_{12}$ (b) alloys at room temperature

without Fe addition contains a single martensite phase shown in Fig. 2(a), which can be indexed to be a ten-layer modulated orthorhombic structure. By contrast, $\text{Ni}_{47}\text{Fe}_3\text{Mn}_{38}\text{Sn}_{12}$ alloys shown in Fig. 2(b) contain a mixture of dual phase: the austenite and γ phase (shown with arrow). The austenite phase can be indexed to be an order cubic $L2_1$ structure. On the other hand, the crystal structure of the γ phase is identified as face-center cubic (FCC) with a space group of $Fm\bar{3}m$ [19]. All above experimental results indicate that by substitution of Fe for Ni, the microstructure and crystal structure of the alloys change at room temperature.

3.2 Martensitic transformation (MT)

The DSC trace for the $\text{Ni}_{50-x}\text{Fe}_x\text{Mn}_{38}\text{Sn}_{12}$ ($x=0$ and 3%) alloys is shown in Fig. 3. There is only one endothermic and exothermic peak during the heating and cooling process, indicating that one-step phase transformation appears in $\text{Ni}_{50-x}\text{Fe}_x\text{Mn}_{38}\text{Sn}_{12}$ ($x=0$ and 3%) alloys. As a kind of typical FSMA, martensitic transformation provides the basic condition and makes it possible to have the practical application of the alloys. Moreover, a tunable MT temperature and a wide MT temperature range are needed. As shown in Fig. 3, the MT temperature decreases notably by substituting a small amount of Fe for Ni. Compared with $\text{Ni}_{50}\text{Mn}_{38}\text{Sn}_{12}$ alloy, the martensitic transformation starting temperature of the $\text{Ni}_{47}\text{Fe}_3\text{Mn}_{38}\text{Sn}_{12}$ alloy is decreased by 32.5 K. The detailed results are given in Table 2. Moreover, it is also

found that the martensitic transformation cover a broad temperature window from 288.9 to 352.2 K. The presented design scheme may be important in exploring multifunctional magneto-responsive materials.

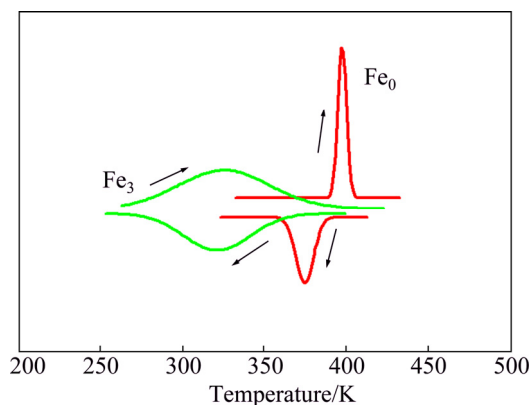


Fig. 3 DSC curves of $\text{Ni}_{50-x}\text{Fe}_x\text{Mn}_{38}\text{Sn}_{12}$ alloys

Table 2 Characteristic temperatures of $\text{Ni}_{50-x}\text{Fe}_x\text{Mn}_{38}\text{Sn}_{12}$ alloys ($x=0$ and 3%)

Alloy	M_s /K	M_f /K	A_s /K	A_f /K
$\text{Ni}_{50}\text{Mn}_{38}\text{Sn}_{12}$	384.7	366.6	394.4	401.3
$\text{Ni}_{47}\text{Fe}_3\text{Mn}_{38}\text{Sn}_{12}$	352.2	288.9	299.2	366.4

3.3 Mechanical properties

The intrinsic brittleness is a critical factor that hinders the engineering application of Ni–Mn–Sn alloys. In order to gain a better appreciation of the mechanical properties, compression tests were conducted at room temperature. Figure 4 shows the mechanical responses of $\text{Ni}_{50-x}\text{Fe}_x\text{Mn}_{38}\text{Sn}_{12}$ alloys at room temperature. The alloys were all loaded until they fractured to observe their compressive strength and ductility. The results in Fig. 4 show that the sample achieves a maximum compressive strength of 855 MPa with a fracture strain of 11%. Compared with $\text{Ni}_{50}\text{Mn}_{38}\text{Sn}_{12}$ alloy, the mechanical properties of the alloy with Fe addition has a significant improvement. In order to investigate the mechanism of the mechanical property improvement, the fracture patterns of $\text{Ni}_{50-x}\text{Fe}_x\text{Mn}_{38}\text{Sn}_{12}$ ($x=0$ and 3%) alloys after compressive test are shown in Fig. 5. It can be seen that, without Fe addition, $\text{Ni}_{50}\text{Mn}_{38}\text{Sn}_{12}$ alloy is brittle. The fracture of $\text{Ni}_{50}\text{Mn}_{38}\text{Sn}_{12}$ alloy is typical intergranular crack of intermetallics. Notably, after Fe addition, some typical transgranular cracks appear and the fracture changes from intergranular fracture to transgranular fracture. The mechanical properties of the alloy are improved. It is also found that the second ductile phases distribute mainly at the grain boundary and thus reduce the intergranular fracture tendency. When the original crack propagates to the boundary between the austenite phase and the second phase, the second phase can be plastically deformed. If the crack traverses the second

phase under a high tensile stress, more energy is needed for the crack propagation, thus resulting in high toughness and ductility. This is the original cause of the significant improvement of the alloy ductility with Fe addition.

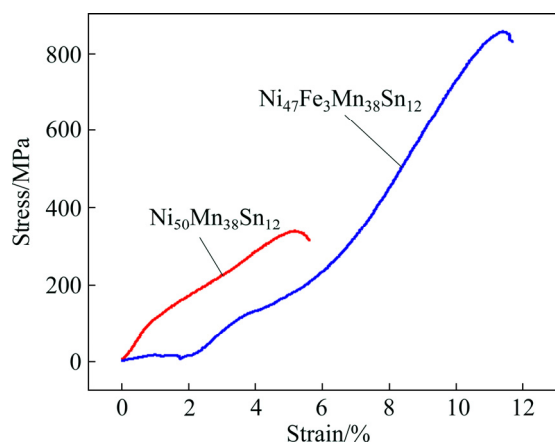


Fig. 4 Compressive stress–strain curves of $\text{Ni}_{50}\text{Mn}_{38}\text{Sn}_{12}$ and $\text{Ni}_{47}\text{Fe}_3\text{Mn}_{38}\text{Sn}_{12}$ alloys at room temperature

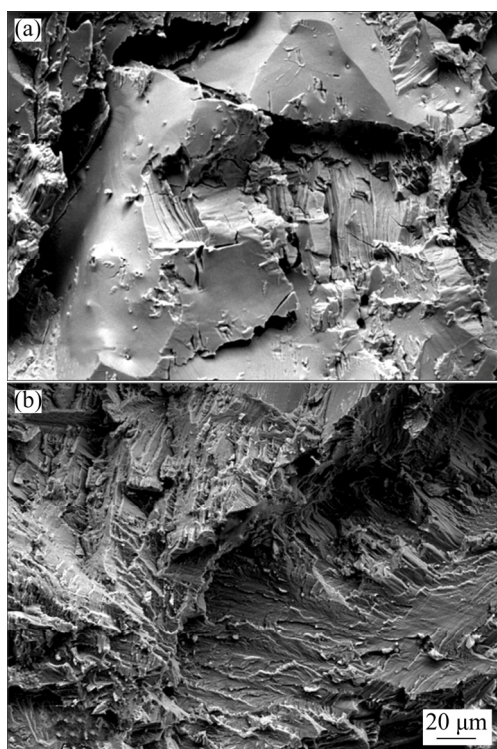


Fig. 5 SEM fractographs of $\text{Ni}_{50}\text{Mn}_{38}\text{Sn}_{12}$ (a) and $\text{Ni}_{47}\text{Fe}_3\text{Mn}_{38}\text{Sn}_{12}$ (b) alloys

4 Conclusions

1) By substitution of Fe for Ni, the crystal structure of the alloys changes at room temperature. It is transformed into the austenitic structure with high symmetry from martensitic structure with low symmetry.

2) The martensitic transformation temperature can be significantly tuned by Fe doping. Compared with

$\text{Ni}_{50}\text{Mn}_{38}\text{Sn}_{12}$ alloy, the martensitic transformation starting temperature of $\text{Ni}_{47}\text{Fe}_3\text{Mn}_{38}\text{Sn}_{12}$ alloy is decreased by 32.5 K. It is also found that martensitic transformation occurs over a broad temperature window from 288.9 to 352.2 K.

3) It is found that the mechanical properties of Ni–Mn–Sn alloy can be significantly improved by Fe addition. The $\text{Ni}_{47}\text{Fe}_3\text{Mn}_{38}\text{Sn}_{12}$ alloy achieves a maximum compressive strength of 855 MPa with a fracture strain of 11%.

4) The mechanism of the mechanical property improvement is clarified. Fe doping changes the fracture type from intergranular fracture of $\text{Ni}_{50}\text{Mn}_{38}\text{Sn}_{12}$ alloy to transgranular cleavage fracture of $\text{Ni}_{47}\text{Fe}_3\text{Mn}_{38}\text{Sn}_{12}$ alloys.

References

- [1] SUTOU Y, IMANO Y, KOEDA N, OMORI T, KAINUMA R, ISHIDA K, OIKAWA K. Magnetic and martensitic transformations of NiMnX (X=In, Sn, Sb) ferromagnetic shape memory alloys [J]. *Applied Physics Letters*, 2004, 85(19): 4358–4360.
- [2] KRENKE T, DUMAN E, ACET M, WASSERMANN E F, MOYA X, MANOSA L, PLANES A. Inverse magnetocaloric effect in ferromagnetic Ni–Mn–Sn alloys [J]. *Nature Material*, 2005, 4(6): 450–454.
- [3] MAÑOSA L, GONZÁLEZ-ALONSO D, PLANES A, BONNOT E, BARRIO M, TAMARIT J L, AKSOY S, ACET M. Giant solid-state barocaloric effect in the Ni–Mn–In magnetic shape-memory alloy [J]. *Nature Materials*, 2010, 9(6): 478–481.
- [4] KAINUMA R, IMANO Y, ITO W, PLANES A, BONNOT E, BARRIO M, TAMARIT J L, AKSOY S, ACET M. Magnetic-field-induced shape recovery by reverse phase transformation [J]. *Nature*, 2006, 439(7079): 957–960.
- [5] LIU Jian, GOTTSCHALL T, SKOKOV K P, MOORE J D, GUTFLEISCH O. Giant magnetocaloric effect driven by structural transitions [J]. *Nature Materials*, 2012, 11(7): 620–626.
- [6] KRENKE T, DUMAN E, ACET M, WASSERMANN E F, MOYA X, MANOSA L, PLANES A, SUARD E, OULADDIAF B. Magnetic superelasticity and inverse magnetocaloric effect in Ni–Mn–In [J]. *Physical Review B*, 2007, 75(10): 4414.
- [7] XUAN Hai-cheng, SHEN Li-juan, TANG Tao, CAO Qing-qi, WANG Dun-hui, DU You-wei. Magnetic-field-induced reverse martensitic transformation and large magnetoresistance in $\text{Ni}_{50-x}\text{Co}_x\text{Mn}_{32}\text{Al}_{18}$ Heusler alloys [J]. *Applied Physics Letters*, 2012, 100(17): 172410–172410-4.
- [8] LI Zhe, JING Chao, CHEN Ji-ping, YUAN Shu-juan, CAO Shi-xun, ZHANG Jin-cang. Observation of exchange bias in the martensitic state of $\text{Ni}_{50}\text{Mn}_{36}\text{Sn}_{14}$ Heusler alloy [J]. *Applied Physics Letters*, 2007, 91(11): 112505–112505-3.
- [9] WANG Bao-min, LIU Y, REN P, XIA B, RUAN K B, YI J B, DING J, LI X G, Wang Lan. Large exchange bias after zero-field cooling from an unmagnetized state [J]. *Physical Review Letters*, 2011, 106(7): 077203.
- [10] XIN Yan, LI Yan. Microstructure and transformation behavior of $\text{Ni}_{54}\text{Mn}_{25}\text{Ga}_{15}\text{Al}_6$ high-temperature shape memory alloy [J]. *Transactions of Nonferrous Metals Society of China*, 2014, 24(1): 126–130.
- [11] TIAN Bin, CHEN Feng, TONG Yun-xiang, LI Ling, ZHENG Yu-feng, LI Qi-zhen. Fracture behavior and structural transition of $\text{Ni}_{46}\text{Mn}_{33}\text{Ga}_{17}\text{Cu}_{4-x}\text{Zr}_x$ alloys [J]. *Materials Science and Engineering*

- A, 2014, 607: 95–101.
- [12] TIAN Bin, CHEN Feng, TONG Yun-xiang, LI Ling, ZHENG Yu-feng. Phase transformation and magnetic property of Ni–Mn–Ga powders prepared by dry ball milling [J]. *Journal of Materials Engineering and Performance*, 2012, 21(12): 2530–2534.
- [13] CASTILLO-VILLA P O, MANOSAET L, PLANES A, FRONTERA C. Elastocaloric and magnetocaloric effects in Ni–Mn–Sn (Cu) shape-memory alloy [J]. *Journal of Applied Physics*, 2013, 113(5): 053506.
- [14] FENG Lin, MA Li, LIU En-ke, WU Guang-heng, WANG W H, ZHANG Wen-xin. Magnetic-field-induced martensitic transformation in MnNiAl:Co alloys [J]. *Applied Physics Letters*, 2012, 100(15): 152401.
- [15] CHEN Feng, WANG Hai-bo, ZHENG Yu-feng, CAI Wei, ZHAO Lian-cheng. Effect of Fe addition on transformation temperatures and hardness of NiMnGa magnetic shape memory alloys [J]. *Journal of Materials Science*, 2005, 40(1): 219–221.
- [16] CZAJA P, SZCZERBA M J, CHULIST R, BAŁANDA M, PRZEWOŹNIK J, CHUMLYAKOV Y I, SCHELL N, KAPUSTA C Z, MAZIARZ W. Martensitic transition, structure and magnetic anisotropy of martensite in Ni–Mn–Sn single crystal [J]. *Acta Materialia*, 2016, 118: 213–220.
- [17] CZAJA P, CHULIST R, SZLEZYNGER M, SKUZA W, CHUMLYAKOV Y I, SZCZERBA M J. Self-accommodated and pre-strained martensitic microstructure in single-crystalline, metamagnetic Ni–Mn–Sn Heusler alloy [J]. *Journal of Materials Science*, 2017, 52(10): 5600–5610.
- [18] WÓJCIK A, MAZIARZ W, SZCZERBA M J, ET AL. Tuning magneto-structural properties of Ni₄₄Co₆Mn₃₉Sn₁₁ Heusler alloy ribbons by Fe-doping [J]. *Materials Science and Engineering B*, 2016, 209: 23–29.
- [19] WU Zhi-gang, LIU Zhi-ping, YANG Hong, LIU Yi-nong, WU Gang, WOODWARD D C. Metallurgical origin of the effect of Fe doping on the martensitic and magnetic transformation behaviours of Ni₅₀Mn_{40-x}Sn₁₀Fe_x magnetic shape memory alloys [J]. *Intermetallics*, 2011, 19(4): 445–452.

Fe 替代 Ni 对 Ni–Mn–Sn 磁性形状记忆合金结构、马氏体相变以及力学性能的影响

谭昌龙¹, 冯志成¹, 张 琨², 吴明阳³, 田晓华¹, 郭二军²

1. 哈尔滨理工大学 应用科学学院, 哈尔滨 150080;

2. 哈尔滨理工大学 材料科学与工程学院, 哈尔滨 150080;

3. 哈尔滨理工大学 高效切削及刀具国家地方联合工程实验室, 哈尔滨 150080

摘 要: 在 Ni_{50-x}Fe_xMn₃₈Sn₁₂ (x=0, 3%, 摩尔分数)铁磁形状记忆合金中, 通过 Fe 元素掺杂部分替代 Ni 元素, 对其结构、马氏体相变以及力学性能的影响进行研究。结果表明, 在室温附近通过 Fe 替代 Ni, 改变了合金的微观组织以及晶体结构, 同时马氏体相变温度下降了 32.5 K。马氏体相变所跨越的温度区间为 288.9~352.2 K。研究发现, 通过掺杂 Fe 元素可以显著提高 Ni–Mn–Sn 合金的力学性能。Ni₄₇Fe₃Mn₃₈Sn₁₂ 合金在 11%断裂应变时展现出最大的压缩强度 855 MPa。另外, 揭示了改善力学性能的机制。通过掺杂 Fe 元素改变了 Ni₅₀Mn₃₈Sn₁₂ 合金晶粒间的断裂方式, 使其从沿晶断裂转变为 Ni₄₇Fe₃Mn₃₈Sn₁₂ 合金的穿晶解理断裂。

关键词: Ni–Mn–Sn 合金; 马氏体相变; 力学性能; 磁性形状记忆合金

(Edited by Bing YANG)